Glass transition of polymers: Memory effects in structural relaxation of polystyrene

S. C. Kuebler, A. Heuer, and H. W. Spiess
Max-Planck-Institut für Polymerforschung, Postfach 3148, D-55 021 Mainz, Germany
(Received 23 May 1996; revised manuscript received 18 March 1997)

The dynamics of the α relaxation in polystyrene is investigated by applying specific multidimensional solid-state NMR echo techniques to evaluate multitime correlation functions. A broad distribution of correlation times characteristic for amorphous polymers above the glass transition temperature is analyzed with respect to temporal fluctuations within the relaxation time distribution. These fluctuations are quantified by a *rate memory parameter* Q. The experimental correlation functions reveal Q to be almost at its theoretical minimum, proving a strong coupling among different relaxation modes. Similar results obtained for polyvinylacetate and ortho-terphenyl indicate that this behavior is a characteristic feature of the dynamics in amorphous systems above the glass transition as seen by NMR experiments. Furthermore, the multitime correlation functions allow one to quantify the heterogeneous and homogeneous contributions to the relaxation process and to determine to what extent the relaxation can be regarded as a heterogeneous superposition of different relaxation processes as opposed to a homogeneous scenario, in which the nonexponentiality is intrinsic. The analysis reveals that the relaxation is close to the heterogeneous limit and that remaining deviations indicate the presence of a small fraction of correlated back-and-forth jumps.
[S1063-651X(97)08407-9]

PACS number(s): 61.43.Fs, 61.41.+e, 64.70.Pf, 05.40.+j

I. INTRODUCTION

Structural relaxation of amorphous materials is often characterized by a nonexponential decay of the measured correlation functions [1], which is attributed to a cooperative, nonlocal dynamics. Numerous models of the cooperativity in glassy materials have been discussed in the literature [2,3] such as the concept of cooperatively rearranging regions [4,5] or the coupling scheme [6]. Additional insight into the nature of the complex dynamics on a microscopic scale can be gained in terms of the concepts of the *relaxation type* and the *rate memory*.

The relaxation type being either heterogeneous or homogeneous is related to the question whether the nonexponentiality is caused by a superposition of different exponential processes or by a superposition of intrinsically nonexponential processes, respectively. Since experimentally accessible correlation functions measure an ensemble average, a distinction between both scenarios cannot be made simply on the basis of the shape of the resulting nonexponential relaxation function. Qualitatively, a heterogeneous relaxation implies the existence of fast and slow segments, attributed to density differences of the local structure [7]. Of course, the density differences as well as the local geometric constraints are not static but fluctuate with time. Therefore, one may speak of *dynamic heterogeneities*. Considering geometric constraints in an amorphous polymer, a preference of correlated back-and-forth jumps may exist even though the molecular potential is not static, but may have changed significantly after a reorientation process. Such effects have indeed been observed in Brownian and molecular-dynamics simulations of polymer chains [8,9]. As shown in Ref. [10], correlated back-and-forth jumps (equivalent to an *orientational memory*) are the origin of homogeneous contributions to the relaxation process. In general, both homogeneous and heterogeneous contributions are expected to be present.

Experimentally, the existence of dynamic heterogeneities has been demonstrated by a number of different experiments [11–15]. To date, however, no experiment has been performed that quantifies the actual contribution of dynamic heterogeneities to the nonexponentiality of the relaxation.

Recently, formal criteria have been proposed that allow us to quantify homogeneous and heterogeneous contributions to the relaxation process from the knowledge of two-time and three-time correlation functions [10]. As will be shown in this paper, these correlation functions are experimentally accessible by multidimensional NMR and allow a determination and quantification of the relaxation type.

The existence of dynamic heterogeneities raises the question of how long a segment may keep its present relaxation rate, introducing the concept of a *rate memory*. Experimentally, a qualitative answer has been sought by means of reduced four-dimensional (4D) exchange NMR spectroscopy, applied to study the α relaxation of polyvinylacetate (PVAC) around the glass transition [11]. The idea behind the experiment (schematically depicted in Fig. 1) is to select a slowly relaxing subensemble and to monitor the time necessary for fluctuations to occur, redistributing these slow segments towards the equilibrium distribution. For PVAC, the time scale of these fluctuations is close to the time scale of the α relaxation itself [16]. Meanwhile, similar observations have been made in reduced 4D experiments on ortho-terphenyl (OTP) [17].

Motivated by the study of Ref. [11], other experimental

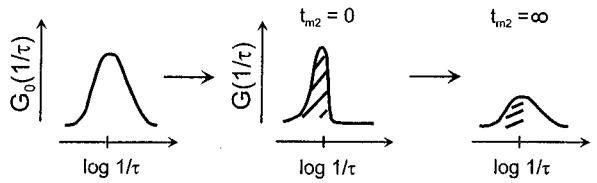

FIG. 1. Principle of experimental techniques to monitor dynamic fluctuations within a distribution of relaxation rates. For example, in 4D NMR, a slow subensemble is selected and its return to the equilibrium distribution with time t_{m2} is monitored.

techniques have been developed to tackle the question of dynamic fluctuations within a relaxation rate distribution. For example, by fluorescence spectroscopy, a dynamically biased subset of probe molecules was selected through photobleaching and the randomization of orientations was pursued by fluorescence decay [18–20]. This experiment will be discussed further in Sec. IV.

It is important to note that information about the rate memory cannot be obtained from measuring two-time correlation functions, e.g., via methods of 2D exchange NMR, yielding a specific rate, but rather by a 4D exchange experiment, capable of relating the rates of a given molecular segment at two different times through the measurement of a four-time correlation function. Consequently, in 2D exchange experiments the relaxation of the entire ensemble is monitored, in contrast to the 4D exchange experiment, which monitors the return of a dynamically biased subensemble into the equilibrium state. Therefore, from the 4D exchange experiments information is obtained that is inaccessible by 2D NMR techniques.

Mathematically, the concept of a rate memory is based on analyzing the possible outcome of a four-time correlation function, accessible through a 4D echo experiment, for a given two-time correlation function as obtained by methods of 2D exchange NMR. Surprisingly, the additional information content of the four-time correlation function can be expressed by a single parameter Q, which can be interpreted as the ratio of typical slow relaxation rates to the average exchange rate between slow and fast segments. Since a strict formulation of the concept of the rate memory is somewhat involved, it is presented in the preceding paper [21].

The present work will focus on a detailed analysis of the dynamic properties of the α relaxation. First, rather than analyzing the four-time correlation function for the limiting case of a bimodal distribution of relaxation rates [16,22] or specific N-state models [17], we demonstrate how the rate memory parameter Q is determined from correlation functions measured in 2D and 4D exchange NMR experiments. Second, we analyze whether the fast fluctuations observed for PVAC are specific to this polymer or are a general feature of the microscopic dynamics of amorphous polymers close to the glass transition. Third, we determine the relaxation type on the basis of the concepts introduced in Ref. [10].

For our present study, we selected amorphous polystyrene (PS), which has been characterized by multidimensional NMR before. From 1D line-shape analysis and 2D exchange experiments, the dynamics of the PS main chain above T_g was described by small-step rotational diffusion with a distribution of correlation times several decades wide and the temperature dependence of the mean correlation times exhibiting a non-Arrhenius temperature dependence [23]. Recently, detailed information about the geometry of main chain motions in PS was obtained by various 3D NMR techniques [24,25]. Two types of motion, namely, small-step reorientations and large angle motions, the latter being associated with conformational transitions [26], were separated.

The paper is organized as follows. After briefly reviewing the relevant aspects of multidimensional solid-state NMR in Sec. II, the theoretical concepts related to the rate memory and the relaxation type are summarized in Sec. III, followed by a discussion of the experimental results in Sec. IV. We conclude with a summary in Sec. V.

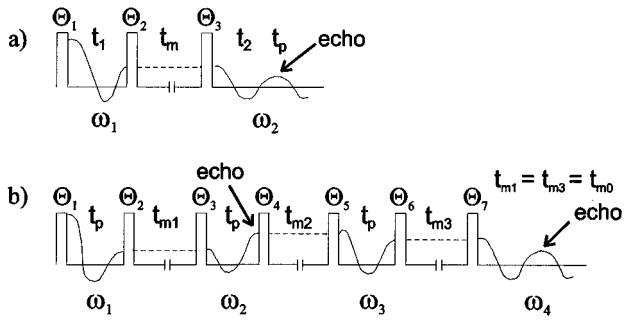

FIG. 2. Schematic view of the pulse sequences for the 2D stimulated echo and 4D echo experiments (see also Table I) to obtain the two-time and four-time correlation functions, respectively. (a) In the stimulated echo experiment, an echo originates from components immobile during t_m, thus measuring the relaxation rate of the entire ensemble. (b) In the 4D echo experiment, molecular segments that are rigid during t_{m1} give rise to a stimulated echo after t_p in the second evolution period. Exchange of reorientation rates may take place during t_{m2}. The same filter is applied during t_{m3}, yielding the final echo intensity in dependence on t_{m2}.

II. ECHO TECHNIQUES IN MULTIDIMENSIONAL SOLID-STATE NMR

Solid-state NMR techniques exploit anisotropic interactions that yield information on the orientation and dynamics of specific molecular sites [27]. For ^{2}H NMR, the spectral shapes are dominated by the coupling of the quadrupole moment of a nucleus to the electric-field gradient at the nuclear site. To a good approximation, the interaction can be described by an axially symmetric field gradient tensor with the unique axis z along the C-^{2}H bond direction, leading to transition frequencies ω:

$$\omega := \omega(\vartheta;t) = \pm\frac{\delta}{2}[3\cos^2\vartheta(t)-1], \tag{1}$$

where δ denotes the anisotropy parameter related to the strength of the quadrupole coupling (typically $\delta = 2\pi\times 125$ kHz for rigid aliphatic C-^{2}H bonds) and $\vartheta(t)$ the time-dependent (due to molecular reorientations) angle between the unique axis of the field gradient tensor and the static magnetic field. Two- and higher-dimensional experiments have been proven particularly useful because the orientations of a C-^{2}H bond can be related at two or more subsequent times. The basic principle of the 2D exchange experiment is outlined in Fig. 2(a). During the evolution time t_1, the angular-dependent frequency of a spin is encoded and is stored with the second pulse as longitudinal magnetization at the beginning of the mixing time t_m. Molecular motions during t_m lead to frequency changes and the new frequency is read out by applying a third pulse, initiating the detection period.

Setting the pulse lengths and phases appropriately [28,29], one obtains the cosine modulated 2D time domain signal, which parametrically depends on the mixing time t_m:

TABLE I. Pulse sequences to measure the different four-time correlation functions; see Eqs. (5) and (6) and Fig. 2(b). The summation of the first and second time domain signals in the table generates the correlation function (5). The correlation function (6) is obtained by summation of all four 4D time domain signals.

4D time domain signal	Θ_1	Θ_2	Θ_3	Θ_4	Θ_5	Θ_6	Θ_7	Receiver
$\langle\cos(\omega_1 t_p)\cos(\omega_2 t_p)\cos(\omega_3 t_p)\cos(\omega_4 t_p)\rangle$	X	X	X	X	X	X	X	Y
$\langle\sin(\omega_1 t_p)\sin(\omega_2 t_p)\cos(\omega_3 t_p)\cos(\omega_4 t_p)\rangle$	X	Y	X	Y	X	X	X	Y
$\langle\cos(\omega_1 t_p)\cos(\omega_2 t_p)\sin(\omega_3 t_p)\sin(\omega_4 t_p)\rangle$	X	X	X	X	X	Y	X	X
$\langle\sin(\omega_1 t_p)\sin(\omega_2 t_p)\sin(\omega_3 t_p)\sin(\omega_4 t_p)\rangle$	X	Y	X	Y	X	Y	X	X

$$F_{2,\cos}(t_1,t_2;t_m)=\langle\cos[\omega(\vartheta;t_m)t_2]\cos[\omega(\vartheta;0)t_1]\rangle, \quad (2)$$

where the angular brackets denote the average over the individual orientations in the sample:

$$\langle\cos[\omega(\vartheta;t_m)t_2]\cos[\omega(\vartheta;0)t_1]\rangle = \int d\vartheta_2 \int d\vartheta_1 \cos[\omega(\vartheta_2;t_m)t_2] \times\cos[(\omega(\vartheta_1;0)t_1]P_{1|1}(\vartheta_2,t_m|\vartheta_1,0)P_{1|0}(\vartheta_1). \quad (3)$$

Here $P_{1|1}(\vartheta_2,t_m|\vartheta_1,0)$ is the conditional probability to find a segment with orientation $\vartheta_2:=\vartheta_2(t_m)$ at a time t_m given it had the orientation $\vartheta_1=\vartheta_1(0)$ at time 0. $P_{1|0}(\vartheta_1)$ is the *a priori* probability to find a segment with orientation ϑ_1. The time domain signal in Eq. (2), when viewed as a function of t_m for given values of t_1 and t_2, can be regarded as a correlation function, which depends parametrically on the values of t_1 and t_2. In this case, we will use the notation $F_{2,\cos}(t_m;t_1,t_2)$ for the correlation function. When focusing on the dynamic properties of a system with identical nuclear sites, it is sufficient to employ echo techniques instead of recording full 2D spectra. Applying the 2D pulse sequence of Fig. 2(a), a stimulated echo originates at a time $t_p:=t_1=t_2$ after the third pulse, caused by segments that did not change their frequency during t_m. Acquiring these echoes as a function of t_m allows Eq. (2) to be rewritten to yield the correlation function [30]:

$$F_{2,\cos}(t_m;t_p)=\tfrac{1}{2}\langle\cos(\omega_2-\omega_1)t_p+\cos(\omega_2+\omega_1)t_p\rangle \cong\tfrac{1}{2}\langle\cos(\omega_2-\omega_1)t_p\rangle, \quad (4)$$

where we have used the abbreviations $\omega_2:=\omega(\vartheta;t_m)$ and $\omega_1:=\omega(\vartheta;0)$ to increase the readability of the formulas here and below. For sufficiently large t_p (typically $\geqslant 30\ \mu$s for rigid deuterons) the last term in the first line of Eq. (4), which corresponds to the free induction decay (FID) starting at time $-t_p$ before the third pulse, has already decayed to zero. Meeting this condition can easily be verified by observing no asymmetry of the echo envelope or, if necessary, the sine modulated correlation function $F_{2,\sin}(t_m;t_p)$ may be added to cancel the unwanted FID, which there appears with a negative sign [30].

From now on we will normalize $F_{2,\cos}(t_m;t_p)$ such that $F_{2,\cos}(t_m=0;t_p)=1$. Furthermore, we will drop the parameter t_p from the argument list of the two-time and four-time correlation functions. For processes with a single correlation time τ_c, the intensity of the stimulated echo decays monoexponentially to a final value dependent on the geometry of the reorientation, i.e., to zero for random jumps in the limit $\delta t_p \gg 1$ [27]. The presence of a distribution of correlation times leads to a nonexponential decay of the stimulated echo and is often accounted for by fitting the decay curve by a stretched exponential according to $F_{2,\cos}(t_m)=\exp[-(t/\tau_0)^\beta]$, with β being a measure for the width of the distribution and τ_0 a characteristic relaxation time [31].

Basically, the pulse sequence for the reduced 4D echo experiment Fig. 2(b), can be viewed as two subsequent stimulated echo experiments, separated by a variable delay time t_{m2}. After the third pulse, a stimulated echo occurs as described above, composed of the C-^{2}H bonds that have not significantly reoriented during the course of the first mixing time. Their magnetization is then stored as longitudinal magnetization in t_{m2}. Thus the first part of the pulse sequence acts as a filter, selecting only components essentially immobile during t_{m1}. During the second mixing time t_{m2}, slow and fast components may exchange due to the fluctuations in the system. Then the same filter is applied in t_{m3} via a second stimulated echo sequence. By selecting pulse lengths and phases accordingly (see Table I and [29]), the following correlation functions are determined as functions of either t_{m1}, t_{m2}, or t_{m3}:

$$F_{4,\cos}(t_{m1},t_{m2},t_{m3})=\langle\cos(\omega_2-\omega_1)t_p\cos(\omega_4 t_p)\cos(\omega_3 t_p)\rangle, \quad (5)$$

where we have already used the shorthand notation introduced above, i.e., $\omega_4:=\omega(\vartheta;t_{m3}+t_{m2}+t_{m1})$. Analogous to the 2D experiment, both the cosine and sine modulated 4D signals can be added to eliminate unwanted contributions, if necessary:

$$F_4(t_{m1},t_{m2},t_{m3})=\langle\cos(\omega_2-\omega_1)t_p\cos(\omega_4-\omega_3)t_p\rangle. \quad (6)$$

To determine fluctuations between fast and slow relaxing segments, the signals $F_{4,\cos}(t_{m1},t_{m2},t_{m3})$ or $F_4(t_{m1},t_{m2},t_{m3})$ are recorded as a function of t_{m2} with t_{m1} and t_{m3} as parameters and we will use $F_{4,\cos}(t_{m2})$ or $F_4(t_{m2})$ for the corresponding correlation functions from now on. Often t_{m1} and t_{m3} are chosen to be equal and will then be denoted t_{m0}. As will be discussed in Sec. IV A, for the determination of the rate memory it is sufficient to employ the signal (5) since the additional measurement of sine terms results only in a small correction to the shape of the echo decay curve. Therefore, in the following, only $F_4(t_{m2})$ will be used to develop the theoretical background, whereas $F_{4,\cos}(t_{m2})$ is measured experimentally to approximate $F_4(t_{m2})$. It is easy to check that mainly components for which $\omega_4=\omega_3$ and $\omega_2=\omega_1$ contribute to the final echo intensity in $F_{4,\cos}(t_{m2})$. Since many segments of the initially selected slow subensemble will have become fast in the limit of long t_{m2}, they will not contribute

to the second stimulated echo acquired after t_{m3}. Therefore, one expects $F_4(t_{m2})$ to decrease monotonically with the mixing time t_{m2} to a final plateau value, which depends on the characteristics of $F_2(t_m)$ and the value of the filter time t_{m_0}, which generally is on the order of τ_0. At this point, it is important to note that whether or not a segment reorients during t_{m2} is not relevant for the final signal intensity since the information not about the orientation of individual segments but rather about their dynamic state is preserved during t_{m2}. As can be seen from Eq. (4), the evolution period parameter t_p is a measure for the angular width of orientations contributing to the stimulated echo intensity [32]. For small t_p, the filter is not very effective, while for large t_p a good orientational selection is possible. Qualitatively, in a 2D exchange spectrum, this corresponds to choosing the bounds for integration of the signal around the diagonal ($\omega_1=\omega_2$) [27]. Note that other mixing times than t_{m2} may be varied as well, resulting in different correlation functions (6). For example, a function $F_4(t_{m3})$, obtained by incrementing t_{m3} for fixed t_{m1} and t_{m2}, will give information about the characteristic relaxation time and width of the correlation time distribution of the selected subensemble. Such studies have been reported previously for polystyrene [12].

III. THEORY

A. Rate memory

In this section we elucidate the additional information content of the four-time correlation function $F_4(t_{m2})$ for a given two-time correlation function $F_2(t_m)$ [21]. In the presence of dynamic heterogeneities, the function $F_4(t_{m2})$ measures the time scale between the limiting cases of no exchange between fast and slow segments for $t_{m2}\rightarrow 0$ and complete exchange for $t_{m2}\rightarrow\infty$, resulting in the equilibrium rate distribution of the whole ensemble.

For the simplest model of a bimodal and equal distribution of relaxation rates, three parameters are involved: a slow and a fast relaxation rate k_s and k_f, as well as an exchange rate Γ between both states. The relaxation of this model as expressed by $F_2(t_m)$ is biexponential with *effective* rates κ_s and κ_f. For $\Gamma\neq 0$, κ_s is greater than k_s, the enhancement being brought about by the exchange process that effectively opens another relaxation channel for an initially slow segment. The effective slow relaxation rate κ_s is then approximately given by $\kappa_s\approx k_s+\Gamma$. Since the value of Γ is only meaningful in comparison to the time scale typical for the whole system, the dimensionless rate memory parameter $Q\geqslant 1$ with

$$Q:=\kappa_s/\Gamma\approx 1+\frac{k_s}{\Gamma}\geqslant 1 \tag{7}$$

is introduced. The rate memory parameter Q counts the number of relaxation processes until a slow segment changes its rate and can simply be expressed on the basis of $F_2(t_m)$ and $F_4(t_{m2})$ since κ_s is obtained from $F_2(t_m)$ and Γ from $F_4(t_{m2})$ [16]. Low-Q values indicate a strong coupling between the different relaxation modes and hence a fast decay of $F_4(t_{m2})$ to its final plateau value and therefore a short-time rate memory, whereas large values of Q are indicative of weak coupling and subsequently a long-time rate memory.

Typically, a continuous rather than bimodal distribution of relaxation rates is observed in amorphous polymers. For this general case a rate memory parameter Q can still be defined, now effectively counting the number of relaxation processes undergone before the present dynamic state of a segment is uncorrelated to its initially slow state. As shown in detail in Ref. [21], $F_4(t_{m2})$ can be calculated on the basis of $F_2(t_m)$ and the experimental parameters t_{m1} and t_{m3} for different values of Q; the relation being in a good approximation

$$F_4(t_{m2})=F_2(t_{m1}+t_{m2}/Q+t_{m3})+\frac{[F_2(t_{m1})-F_2(t_{m1}+t_{m2}/Q)][F_2(t_{m3})-F_2(t_{m3}+t_{m2}/Q)]}{1-F_2(t_{m2}/Q)}. \tag{8}$$

We note here that this equation is expected to hold particularly well if the homogeneous contributions are small and $t_{m1}=t_{m3}$; see Sec. V B of Ref. [21].

The dependence of Eq. (8) on all three mixing times t_{m1}, t_{m2}, and t_{m3} might suggest that Q can also be extracted by variation of t_{m1} or t_{m3} for a fixed value of t_{m2}. However, as will be illustrated by an experimental example, this cannot be recommended in practice.

B. Relaxation type

As already discussed in the Introduction, the relaxation type describes whether the nonexponentiality is mainly due to heterogeneous (superposition of different exponential relaxation processes) or homogeneous (superposition of identical intrinsically nonexponential relaxation processes) dynamics. As shown in [10], intrinsically nonexponential dynamics can be uniquely traced back to the presence of correlated back-and-forth jumps. Hence both limits can be characterized so that in the heterogeneous case there are *no* back-and-forth jumps and in the homogeneous case *no* slow and fast segments, i.e., no selectivity. Verifying the occurrence of back-and-forth jumps requires the knowledge of the orientation of a given segment at at least three successive times. Therefore, the measurement of a three-time correlation function is necessary to determine the relaxation type. Specifically, the measurement of the particular three-time correlation function

$$\langle\cos(\omega_3-\omega_2)t_p\cos(\omega_2-\omega_1)t_p\rangle \tag{9}$$

is required, which appears to be accessible by means of the 3D exchange pulse sequence. A closer examination, however, yields that all four 3D time domain signals need to be measured and combined in an experimentally infeasible fash-

ion [33]. Yet the structure of the required three-time correlation function is identical to the four-time correlation function F_4 of Eq. (6) under the condition that $\omega_3=\omega_2$ in the latter. Therefore, the three-time correlation function can be realized by means of a 4D exchange experiment since the condition $\omega_3=\omega_2$ can be assured by setting t_{m2} to the smallest experimentally possible value (usually $\cong 1$ ms), excluding the occurrence of molecular reorientation in this time period. As will be shown below, $F_4(t_{m1},t_{m2},t_{m3})$ will be evaluated for particular values of $t_{m1}=t_{m3}=t_{m0}/2$, that is,

$$F_4(t_{m1}=t_{m0}/2,t_{m2}=0,t_{m3}=t_{m0}/2) = \langle \cos(\omega_2-\omega_1)t_p \cos(\omega_4-\omega_3)t_p \rangle \qquad (10)$$

will be measured, where the notation $t_{m2}=0$ is meant to indicate the shortest experimentally possible value for the respective mixing time, ensuring that the condition $\omega_3=\omega_2$ is met. In the following, we will use the notation $F_4(t_{m1},t_{m3})$ for the special three-time correlation function to preserve its close relation to the actual 4D experiments, performed for the shortest possible value of t_{m2}.

In the homogeneous case, a subensemble is always indistinguishable from the entire ensemble, rendering the filter selection ineffective, with the result that the outcome after the mixing time t_{m3} is independent from the events during the first mixing time t_{m1}. Thus the following factorization is allowed:

$$F_4(t_{m1},t_{m3})=F_2(t_{m1})F_2(t_{m3}), \qquad (11)$$

which establishes a condition for the homogeneous case [10].

In contrast, the condition for the heterogeneous case is obtained by considering the total absence of back-and-forth jumps. Back-and-forth jumps do not contribute to $F_4(t_{m1},t_{m3})$ since any segment that moves significantly during t_{m1} and jumps back during t_{m3} does not pass the first filter and thus does not contribute to $F_4(t_{m1},t_{m3})$. It will, however, contribute to $F_2(t_m)$ with $t_m=t_{m2}+t_{m3}$ since the orientation at $t=0$ and $t=t_m$ is the same. Consequently, only in the limit of a vanishing probability of correlated back-and-forth jumps are the correlation functions $F_2(t_m)$ and $F_4(t_{m1},t_{m3})$ expected to be equal. Specifically, the condition for the heterogeneous case reads

$$F_4(t_{m1},t_{m3})=F_2(t_{m1}+t_{m3}). \qquad (12)$$

Mathematically, this relation is equivalent to the statement $\langle \sin(\omega 2-\omega_1)t_p \sin(\omega_4-\omega_3)t_p \rangle=0$ [10]. Generally, if both homogeneous and heterogeneous contributions are present, one expects (see [10])

$$[F_2(t_{m0}/2)]^2 \leqslant F_4(t_{m0}/2,t_{m0}/2) \leqslant F_2(t_{m0}). \qquad (13)$$

In the case of purely homogeneous relaxation the first two functions are identical, whereas for purely heterogeneous relaxation the second and the third function are identical. Hence a comparison of the three functions directly allows one to judge whether homogeneous or heterogeneous relaxation predominates. The experimental realization to determine the relaxation type by applying Eq. (13) will be discussed in Sec. IV.

Originally, in Ref. [10] the formalism was developed and applied to the case of translational dynamics, but can be transferred to rotational dynamics as well. In this case two rather subtle complications arise. The first is related to the fact that the range of ω is finite ($-\delta/2 \leqslant \omega \leqslant \delta$). A segment, that by chance changed its NMR frequency from $-\delta/2$ to δ during the first time interval will afterward experience a negative change in frequency. This appear like a correlated back-and-forth jump in frequency space since $\omega_1-\omega_2)(\omega_3-\omega_4)<0_1$. Although the jump processes may occur without any orientational memory, according to our definition, this results in homogeneous contributions. Correlations of this kind, albeit somewhat weaker, will also hold for less extreme cases. They can be reduced by choosing sufficiently large values of t_p since then such correlations are effectively smeared out. The second complication is due to the nonlinear dependence of the NMR frequency on orientation; see Eq. (1). This means that for some orientations a jump of, e.g., 10 ° leads to a significant change in ω, whereas for some other orientations ω will basically remain constant. In terms of the above definitions this will be interpreted as the first segment being ''faster'' (in terms of the change in ω) than the second, leading to small heterogeneous contributions, even if both segments exhibit identical dynamics. This effect can equally be circumvented by increasing the value of t_p, thereby effectively increasing the ''strength'' of the filter and thus its ability to be sensitive to small frequency changes. Only for the case that the dynamics strictly corresponds to rotational diffusion, such as for the dynamics of colloids, the situation is not alleviated by increasing the value of t_p [34].

IV. RESULTS AND DISCUSSION

A. Experiment

Polystyrene, deuterated at the main chain $(PS-d_3)_1$ was purchased from Polymer Standards Service, Mainz, Germany. The sample had a weight average molecular weight of 173 000 g/mol and a polydispersity value of 1.03. The glass transition temperature obtained by differential scanning calorimetry was 376 K with a heating rate of 10 K/min. ^{2}H NMR spectra were recorded on a Bruker CXP 300 spectrometer, operating at a resonance frequency of 45 MHz with a 90° pulse length of 3 μs. The recycle delay was set to 3 s, which was at least three times longer than the longitudinal relaxation time. The total experimental time ranged between several hours for the stimulated echo decays and $2-3$ days for a 4D experiment. The sample was annealed for at least 6 h prior to the experiments; during the measurements the temperature stability was better than ± 0.5 K.

B. Rate memory

The NMR experiments on polystyrene were performed at temperatures above T_g where the average correlation times are in the slow-motion limit (1 ms $\leqslant \tau_c <$ 10 s). The data obtained from the stimulated echo decay $F_{2,\cos}(t_m)$ measured at $T=T_g+10$ K are shown in Fig. 3(a). The evolution time was set to $t_p=30$ μs to provide efficient filtering. Both the cosine and the sum of the cosine and sine modulated 2D data sets were recorded to test the assumption in Eq. (3); virtually identical parameters were obtained in both cases. The solid line is a fit of a stretched exponential with the characteristic

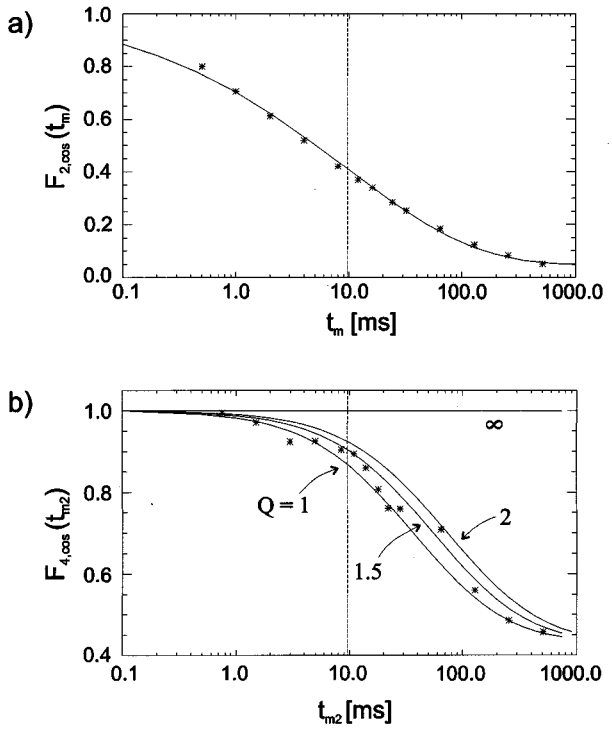

FIG. 3. (a) 2D echo decay $F_{2,\cos}(t_m)$ for polystyrene at $T=T_g+10$ K with $t_p=30$ μs. The solid line represents a stretched exponential with fit parameters $\beta=0.38$ and $\tau_0=9.5$ ms. (b) 4D echo decay $F_{4,\cos}(t_{m2})$ obtained with the filter t_{m0} set to 15 ms. The theoretical curves for different Q calculated from the 2D echo data are also shown. For $Q=1$, the information of the initial rate is lost after a single relaxation process, whereas $Q\rightarrow\infty$ corresponds to the maximum rate memory. The experimental data indicate Q to be near the theoretical minimum of $Q=1$, implying strong fluctuations between slow and fast segments. $F_{4,\cos}$ has been normalized so that $F_{4,\cos}(0)=1$.

time constant τ_0 of 9.5 ms and a distribution constant $\beta=0.38$. The parameters correspond to an average correlation time of $\langle\tau_c\rangle=(\tau_0/\beta)\Gamma(1/\beta)=37$ ms and to a distribution of relaxation rates with a full width at half maximum of about 3 decades. The longitudinal relaxation time measured independently could be approximated as a single exponential with $T_1=800$ ms and, together with the prefactor of the fitting function, was used to normalize the 2D echo decay. The values are in agreement with previous data obtained by NMR [23] and those obtained by light scattering techniques [35,36].

In the 4D echo experiment, $t_{m1}=t_{m3}=t_{m0}$ was set to 15 ms to achieve a good filter effect within the relaxation rate distribution and to apply the same filter before and after the second mixing time. A smaller value of t_{m0}, which is best chosen to be on the order of τ_0, results in an insufficient filter, whereas for longer values of t_{m0}, most of the signal intensity is discarded by the first filter, thus causing signal-to-noise problems in the subsequent analysis. As in the 2D experiment, t_p was set to 30 μs. The experimental 4D echo decay, normalized to its value for the shortest mixing time t_{m2}, is presented in Fig. 3(b). The data were corrected for longitudinal relaxation with an exponential decay with $T_1=1.1$ s.

It is immediately visible that the relaxation rate of the selected subensemble is slower than that of the entire ensemble. The rate memory, however, is not infinite since $F_{4,\cos}(t_{m2})$ decays with time, indicating equilibration of the subensemble in a finite time as one would expect for any ergodic system. Theoretical curves for $F_{4,\cos}(t_{m2})$ for different values of Q, calculated from Eq. (8), are shown as solid lines. A comparison with the experimental data reveals Q to be between 1 and 1.5, whereas the calculated curve for $Q=2$ already shows significant deviations from the experimental data points. The small value of Q indicates that a selected, initially slow segment needs only between one and two elementary steps to become equilibrated again, which is close to the theoretical minimum of $Q=1$.

One experimental uncertainty in the determination of Q is given by the possibility to normalize the NMR data to the value of the shortest mixing time t_{m2}. Therefore, it is important to measure at temperatures not too high so that τ_0 is long enough to determine the initial plateau value. In the present experiment, the normalization leads to insignificant variations for the value of Q only. Furthermore, in multidimensional exchange NMR, the exchange intensity (or, equivalently, the reduction in the echo intensity) may arise not only from dynamic processes, but also from spin diffusion, that is, magnetization transfer among ^{2}H nuclei mediated by dipole-dipole couplings. In the past, the effect of spin diffusion has been ruled out from the observed temperature dependence of the exchange process, assuming spin diffusion to be a non-thermally activated process. For PS, it has been shown by 2D exchange NMR below T_g that the time constant for spin diffusion is more than 100 s [37]. Recent investigations have addressed the question whether molecular motions have an impact on the spin diffusion rates in deuterated systems [38,39]. There it was concluded that for disordered systems close to the glass transition with motional correlation times of the order of $10^{-3}-1$ s (slow motion limit), as studied here, the effects of spin diffusion can be neglected in analyzing stimulated echo decay functions. For $\tau_c>1$ s, spin diffusion processes (with typical time constants of tens of seconds) compete with dynamic processes. Additionally, for rigid systems, spin diffusion rates are only nonzero for small frequency separations (less than 5–10 kHz). Yet motions with τ_c in the range 10^{-6}–10^{-3} s can render the spin diffusion rates temperature dependent, resulting in spin diffusion rates in the range $1–10\,s^{-1}$ [39]. As can be seen from Fig. 3(b), the value of Q is determined from the part of the decay curves where $t_m\leqslant 200$ ms [note that $F_4(t_{m2})$ scales logarithmically with Q in the plots; cf. Ref. [21]]. In this time regime, experimental implications such as relaxation and spin diffusion are negligible.

Since the theoretical curve for $F_{4,\cos}(t_{m2})$ is calculated from experimentally obtained values for $F_{2,\cos}(t_{tm})$, the dependence of the value of Q on the stimulated echo fit parameters needs to be determined. The experimental $F_{2,\cos}(t_m)$ data in Fig. 4(a) can be reasonably well fitted with β ranging from 0.3 to 0.4 and τ_0 between 7 ms and 10 ms, respectively. The calculated curves for $F_{4,\cos}(t_{m2})$ corresponding to those parameters are shown in Fig. 4(b). The slope is only slightly influenced, with variations on the order of the experimental

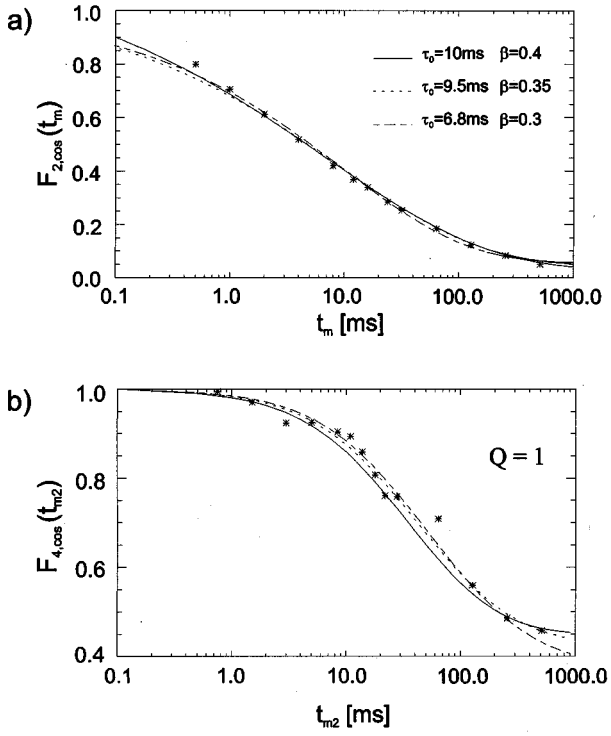

FIG. 4. Analysis of the influence of the 2D fit parameters on the calculation of $F_{4,\cos}(t_{m2})$ for $Q=1$. (a) $F_{2,\cos}(t_m)$ for reasonable fits with β in the range 0.3–0.4 and relaxation constants τ_0 between 7 and 10 ms. (b) $F_{4,\cos}(t_{m2})$ determined on the basis of the 2D functions in (a). The calculated decays are only slightly influenced by variation of the fit parameters.

uncertainties. Accordingly, Q does not depend crucially on the choice of the fit parameters of the 2D echo data.

Unfortunately, the temperature dependence of Q cannot be obtained from multidimensional NMR experiments since for most polymers the slow motion limit assumption, where the analysis is applicable, is valid only up to approximately T_g+25 K. Simulations on the basis of a modified Fredrickson model, where such restrictions do not exist, indicate a weak temperature dependence of Q [40].

A similar small value of Q was found for PVAC at T_g+20 K [16], which is close to the minimum value of $Q\cong 1$ observed in polystyrene, indicating large dynamic fluctuations and intimately coupled relaxation modes near the glass transition. Since in the meantime a similar result has even been found for a low-molar glass-forming system [17], it seems that by analyzing fluctuations in terms of a rate memory parameter we have found a behavior that is typical for strongly cooperative motion around the glass transition.

Comparing the results of the 4D NMR experiments on amorphous polymers with those obtained by other spectroscopic techniques, it is striking that the photobleaching experiments performed on the low-molar glass-former OTP indicates that there is a large fraction of probe molecules that, initially slow, do not randomize during a time period considerably larger than the average reorientation rate [20]. These long-lived constraints would indicate a large value of Q, in marked contrast to the 4D NMR experiments performed on OTP, which can also be modeled well in terms of a minimum rate memory [17]. Since these discrepancies point towards an effect that is interesting and so far not understood, we briefly mention some major differences between both experiments. (i) In NMR, the sample itself is deuterated, while the optical technique relies on a fluorescent probe molecule which, however, has been shown to follow the bulk dynamics very well. (ii) In the fluorescent experiments, the depth of the bleaching as set by the laser beam determines the filter strength. The effectiveness of the bleaching has been observed to depend strongly on the experimental conditions, such as the probe molecule and the system under investigation in an *a priori* unknown way. In contrast, the stimulated echo filter in the 4D NMR experiment is quantitatively set by the time delay t_{m0}. (iii) The optical experiment has been performed exactly at T_g (10–20 K lower than the NMR experiment).

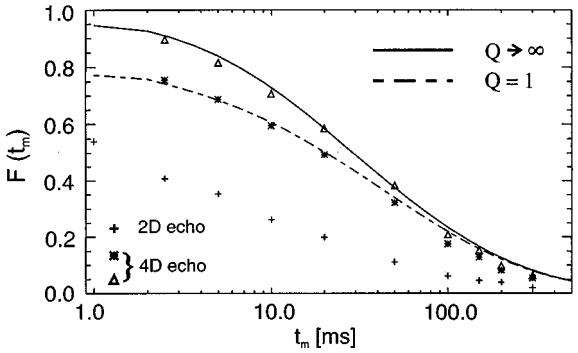

FIG. 5. 2D echo decay in PS and theoretical prediction of the 4D echo decay dependent on t_{m3} in terms of the rate memory for $Q\rightarrow\infty$ (solid line) and $Q\rightarrow 1$ (dashed line). Both experimental curves $F_4(t_{m3})$ differ only by a scaling factor. This demonstates that experimentally Q cannot be extracted from the variation of t_{m3}.

Finally, we address the question of whether sampling of t_{m3} for fixed t_{m1} and t_{m2} is capable of obtaining the rate memory parameter Q. To this end, the data obtained previously for PS [12] were reanalyzed; see Fig. 5. The 2D echo decay is characterized by $\tau_0=5$ ms and $\beta=0.33$, whereas the selected slow subensemble has a characteristic time constant about five times longer with a narrower distribution parameter β. It turns out that the different theoretical curves for $Q=1$ and $Q=\infty$ are rather similar as compared to the significant differences one would obtain from variation of the central mixing time t_{m2}. As also shown in Fig. 5, by appropriate scaling both limiting cases $Q=1$ and $Q=\infty$ fit the data equally well so that in practical applications no statement about the rate memory can be made. Since for typical experimental parameters $F_4(t_{m2})$ displays a plateau value for small t_{m2} the normalization problem does not occur when varying t_{m2} rather than t_{m3}. The situation is slightly better in simulations since in contrast to the NMR experiment the data point for $t=0$ can be determined so that no additional scaling has to be taken into account [10].

C. Relaxation type

To determine whether the dynamics in PS is mainly heterogeneous or homogeneous based on Eq. (13) we measured $F_{2,\cos}(t_m)$, shown in the upper curve in Fig. 6. Fitting a stretched exponential yields $\tau_0=6.5$ ms and $\beta=0.45$ for

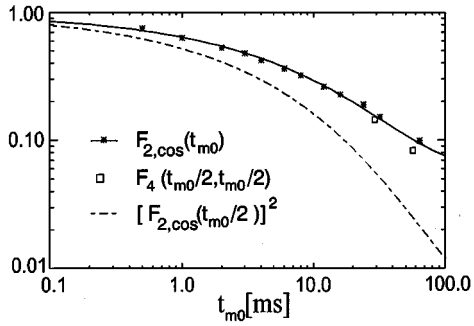

FIG. 6. Determination of the relaxation type for PS at $T=T_g+13$ K. The close agreement between $F_4(t_{m0}/2,t_{m0}/2)$ and $F_{2,\cos}(t_{m0})$ indicates that the dynamics is mainly heterogeneous. However, the small deviations indicate some fraction of correlated back-and-forth jumps.

$F_{2,\cos}(t_m)$. The temperature ($T=T_g+13$ K) was slightly higher than for the previous measurements, accounting for the reduced distribution width of correlation times at higher temperatures observed previously for PS-d_3 [23]. From $F_{2,\cos}(t_m)$ the dashed line representing $[F_{2,\cos}(t_m/2)]^2$ was calculated. The four-time correlation function $F_4(t_{m0}/2,t_{m0}/2)$ was measured for $t_{m0}=4.3\tau_0$ and $t_{m0}=8.7\tau_0$.

Here one experimental aspect has to be taken into account. Note that different pulse sequences were applied to obtain $F_{2,\cos}(t_{m0})$ and $F_4(t_{m0}/2,t_{m0}/2)$ and therefore the absolute value of $F_{2,\cos}(t_{m0})$ measured via a 2D echo experiment cannot be compared directly to the value for $F_4(t_{m0}/2,t_{m0}/2)$ acquired by applying a 4D echo sequence. Comparability for the two values of t_{m0} given above can be achieved by measuring $F_4(t_{m0},0)$, that is, a 4D echo experiment with either t_{m1} or t_{m3} is set to t_{m0} and the remaining two mixing times are set to the shortest possible value (1 ms). This allows one to normalize the intensities obtained for $F_4(t_{m0}/2,t_{m0}/2)$ according to $F_4(t_{m0}/2,t_{m0}/2)F_{2,\cos}(t_{m0})/F_4(t_{m0},0)$. Note that rather than $F_{4,\cos}(t_{m0}/2,t_{m0}/2)$, $F_4(t_{m0}/2,t_{m0}/2)$ was measured to eliminate even the slightest influence of the second term in Eq. (2) on the intensity of the echoes in $F_4(t_{m0}/2,t_{m0}/2)$.

The close agreement between $F_4(t_{m0}/2,t_{m0}/2)$ and $F_{2,\cos}(t_{m0})$ indicates that the relaxation is mainly heterogeneous; cf. Eq. (13). However, there are small but significant deviations revealing some homogeneous contributions. By simulations and analytical calculations it has been checked that the homogeneous contributions that arise as a trivial NMR effect (see Sec. III) only partly contribute to this difference. Hence the experimental data indicate a finite fraction of correlated back-and-forth jumps. A quantitative analysis of this aspect will be presented elsewhere.

V. SUMMARY

We showed that a model-free interpretation of higher-order correlation functions determined by NMR reveals important information about the complex dynamics close to the glass transition. We analyzed quantitatively the microscopic dynamic properties of polymer segments by relating experimental data to a theoretical description of dynamic fluctuations of both the orientation and the probability for changing the orientation. This has been achieved by applying the theoretical concepts of rate memory and relaxation type. The characteristic time of a crossover between a slow and a fast relaxing subensemble was determined via multidimensional NMR by analyzing a four-time correlation function. The information content of the four-time correlation function as compared to a two-time correlation function can be parametrized by a single parameter Q, which is a measure for the rate memory, and the additional information content of $F_4(t_m)$ can be obtained without assuming a particular functional form of $F_2(t_m)$. The experimental value of Q for polystyrene is near its theoretical minimum, implying a maximal fluctuation rate within a rate distribution of given width. This observation is similar to the results for polyvinylacetate and ortho-terphenyl, suggesting a common behavior of reorientation dynamics of glass-forming systems above T_g with respect to the rate memory but deviates from the optical experiments. Additionally, simulations of a generalized Fredrickson model, which is a rather simple spin lattice model, also reveal values of Q close to 1 [40].

Furthermore, the relaxation is mainly heterogeneous with only very small homogeneous contributions, indicating a small fraction of correlated back-and-forth jumps. The dominance of heterogeneous contributions is in marked contrast to, e.g., the translational dynamics of a polymer melt far above the glass transition. There it has been shown via computer simulations that the dynamics is mainly homogeneous [10], as already predicted by the Rouse model of polymer dynamics [42,10]. Only close the glass transition the dynamics becomes apparently heterogeneous, indicating deviations from the Rouse model.

ACKNOWLEDGMENTS

We thank Dr. D. J. Schaefer for valuable discussions and carefully checking the manuscript. We gratefully acknowledge discussions with U. Tracht as well as with Professor H. Sillescu and his group. Financial support has been provided by the Deutsche Forschungsgemeinschaft (SFB 262/D10).

[1] N. G. McCrum, B. E. Read, and G. Williams, *Anelastic and Dielectric Effects in Polymeric Solids* (Wiley, New York, 1967).
[2] J. Jäckle, Rep. Prog. Phys. **49**, 171 (1986).
[3] Proceedings of the International Discussion Meeting on Relaxation in Complex Systems II, edited by K. L. Ngai, E. Riande, and G. B. White [J. Non-Cryst. Solids **172-174** (1994)].
[4] G. Adam and J. H. Gibbs, J. Chem. Phys. **28**, 373 (1965).
[5] E. J. Donth, J. Non-Cryst. Solids **53**, 325 (1982).
[6] K. L. Ngai and C. T. White, Phys. Rev. B **20**, 2425 (1979).
[7] F. Fujara, B. Geil, H. Sillescu, and G. Fleischer, Z. Phys. B **88**, 195 (1992).

[8] E. Helfand, Z. R. Wasserman, and T. A. Weber, Macromolecules **13**, 526 (1980).
[9] H. Takeuchi and R.-J. Roe, J. Chem. Phys. **94**, 7446 (1991); **94**, 7458 (1991).
[10] A. Heuer and K. Okun, J. Chem. Phys. **106**, 6176 (1997).
[11] K. Schmidt-Rohr and H. W. Spiess, Phys. Rev. Lett. **66**, 3020 (1991).
[12] J. Leisen, K. Schmidt-Rohr, and H. W. Spiess, Physica A **201**, 79 (1993).
[13] C. T. Moynihan and J. Schroeder, J. Non-Cryst. Solids **160**, 52 (1993).
[14] R. Richert, Macromolecules **21**, 923 (1988).
[15] B. Schiener, A. Loidl, R. Böhmer, and R. V. Chamberlin, Science **274**, 752 (1996).
[16] A. Heuer, M. Wilhelm, H. Zimmermann, and H. W. Spiess, Phys. Rev. Lett. **75**, 2851 (1995).
[17] R. Böhmer, G. Hinze, G. Diezemann, B. Geil, and H. Sillescu, Europhys. Lett. **36**, 55 (1996).
[18] M. T. Cicerone, F. R. Blackburn, and M. D. Ediger, Macromolecules **28**, 8224 (1995).
[19] M. T. Cicerone, F. R. Blackburn, and M. D. Ediger, J. Chem. Phys. **102**, 471 (1995).
[20] M. T. Cicerone and M. D. Ediger, J. Chem. Phys. **103**, 5684 (1995).
[21] A. Heuer, preceding paper, Phys. Rev. E **XX**, XXX (1997).
[22] H. Sillescu, J. Chem. Phys. **104**, 4877 (1996).
[23] U. Pschorn, E. Rössler, H. Sillescu, S. Kaufmann, D. Schaefer, and H. W. Spiess, Macromolecules **24**, 398 (1991).
[24] J. Leisen, K. Schmidt-Rohr, and H. W. Spiess, J. Non-Cryst. Solids **172-174**, 737 (1994).
[25] A. Heuer, J. Leisen, S. C. Kuebler, H. W. Spiess, J. Chem. Phys. **105**, 7088 (1996).
[26] K. Zemke, B. F. Chmelka, K. Schmidt-Rohr, and H. W. Spiess, Macromolecules **24**, 6874 (1991).
[27] K. Schmidt-Rohr and H. W. Spiess, *Multidimensional Solid State NMR and Polymers* (Academic, London, 1994).
[28] C. Schmidt, B. Blümich, and H. W. Spiess, J. Magn. Reson. **79**, 390 (1988).
[29] D. Schaefer, J. Leisen, and H. W. Spiess, J. Magn. Reson. A **115**, 60 (1995); D. Schaefer, Ph.D. thesis, University of Mainz, 1992 (unpublished).
[30] H. W. Spiess, J. Chem. Phys. **72**, 6755 (1980).
[31] C. P. Lindsey and G. D. Patterson, J. Chem. Phys. **73**, 3348 (1980).
[32] F. Fujara, S. Wefing, and W. F. Kuhs, J. Chem. Phys. **88**, 6801 (1988).
[33] S. C. Kuebler, Ph.D. thesis, University of Mainz, 1996 (unpublished).
[34] R. Böhmer, G. Hinze, G. Diezemann, and H. Sillescu (unpublished).
[35] C. P. Lindsey, G. D. Patterson, and J. R. Stevens, J. Polym. Sci. Polym. Phys. Ed. **17**, 1547 (1979).
[36] G. D. Patterson, C. P. Lindsey, and J. R. Stevens, J. Chem. Phys. **70**, 643 (1979).
[37] S. Kaufmann, S. Wefing, D. Schaefer, and H. W. Spiess, J. Chem. Phys. **93**, 197 (1990).
[38] G. Diezemann, J. Chem. Phys. **103**, 6368 (1995).
[39] A. Müller and U. Haeberlen, Chem. Phys. Lett. **248**, 249 (1996); A. Müller, H. Zimmermann, and U. Haeberlen, J. Magn. Reson. A (to be published).
[40] A. Heuer, U. Tracht, and H. W. Spiess (unpublished).
[41] A. S. Kulik, H. W. Beckham, K. Schmidt-Rohr, D. Radloff, U. Pawelzik, C. Boeffel, and H. W. Spiess, Macromolecules **27**, 4746 (1994).
[42] M. Doi and S. F. Edwards, *The Theory of Polymer Dynamics* (Oxford Science, Oxford, 1986).